
ARTICLE

Thermal Properties of UO_2 by Molecular Dynamics Simulation

Tepei UCHIDA^{1,*}, Takeo SUNAOSHI², Masato KATO¹ and Kenji KONASHI³

¹ Japan Atomic Energy Agency, 4-33 Muramatsu, Tokai-mura, Naka-gun, Ibaraki-ken, 319-1194, Japan

² Inspection Development Company Ltd, 4-33 Muramatsu, Tokai-mura, Naka-gun, Ibaraki-ken, 319-1194, Japan

³ Tohoku-University, 2145-2 Narita-cho, Oarai-machi, Higashi-ibaraki-gun, Ibaraki, 311-1313, Japan

Molecular dynamics (MD) simulation was performed to investigate thermal expansion, specific heat and thermal conductivity of UO_2 . For thermal expansion, experimental measurements were made and compared with MD simulation results. These thermal expansion values and other reported data were in good agreement with the MD thermal expansion value. Effects of Schottky defects on thermal properties were evaluated. For thermal expansion, the effect was negligible. For specific heat, the constant volume term of specific heat increased with increasing Schottky defect concentration. But the dilation term of specific heat was nearly-unchanged. Thermal conductivity decreased with increasing Schottky defect concentration. It was considered that the increasing constant volume term was caused by increasing internal energy which was attributed to the Schottky defects. Calculated thermal conductivity values corresponded to experimental data when the supercell contained Schottky defects. It was thought that a perfect crystalline supercell caused high thermal conductivity and the defect structure scattered phonon vibrations and decreased the thermal conductivity.

KEYWORDS: thermal expansion, specific heat, thermal conductivity, molecular dynamics simulation, dilatometer, Schottky defect, UO_2

I. Introduction

Experiments on physical properties of mixed oxide (MOX) fuel and minor actinides (MAs: Np, Am, Cm) containing MOX fuel for fast reactor have been made to evaluate effects of various parameters such as temperature, plutonium contents and oxygen-to-metal (O/M) ratio. Thermal conductivity and melting point are especially significant for designing nuclear fuels. Thermal expansion is also a significant property for thermal design of nuclear fuels, especially with reference to evaluation of pellet-cladding mechanical interaction. In addition, the coefficient of thermal expansion is required to evaluate other thermal properties.

In parallel with experiments, molecular dynamics (MD) simulation has been developed to evaluate validities of experimental data and to predict thermal properties. MD simulation can also calculate nonmeasurable thermal properties, and evaluate relativity between composition and macro properties.

In this study, MD simulation was used to investigate thermal expansion, specific heat and thermal conductivity of UO_2 which is the mother phase of MOX fuel. Effects of Schottky defects which are generated in a lattice on the thermal properties were evaluated. In addition, thermal expansion measurements on UO_2 were carried out for temperature from 300 K to 1923 K. The obtained data was compared with reported bulk expansion data and lattice expansion data.

II. Thermal Expansion Measurement

1. Specimen Preparation

The starting material was UO_2 raw powder. The powder was prepared by calcination in Ar/H_2 gas atmosphere to control its O/M ratio at 2.0. The calcined powder was pressed into a pellet shape with binder, which was coated on the inside of the die, and then sintered at 1923 K for 3 hours in Ar/H_2 atmosphere. Dimensions of a sintered pellet were 10.663 mm in height x 4.227 mm in diameter. Density of the pellet was 10.53 g/cm^3 and its theoretical density was 96.08%.

2. Experimental Details

Linear thermal expansion (LTE) measurements were conducted on the UO_2 pellet using a dilatometer (Bruker AXS, TD5200SA). LTE is given by $\Delta L/L \times 100$, where L is the height dimension at a standard temperature, and ΔL is the expansion of height from that at the standard temperature. LTE measurements were made at 200 K intervals and the specimen was kept at the measurement temperature for 60 min. LTE measurements with increasing temperature were difficult, because it was uncertain that thermal expansion of the heated pellet had reached equilibrium at the temperature. The atmosphere during heating was controlled by flowing Ar/H_2 gas to keep the O/M ratio stoichiometric. Non-reversible shrinkage or expansion of a pellet did not occur.

III. Molecular Dynamics Simulation

1. Interatomic Potentials

The "Materials explorer" program developed by Fujitsu,

* Corresponding author, Email: uchida.tepei@jaea.go.jp

Inc. was used for MD simulations. Born-Mayer-Huggins interatomic potential with the partially ionic model added Morse potential to each ion pair was employed. The interatomic potential function is shown by

$$U_{ij}(r_{ij}) = \frac{z_i z_j e^2}{4\pi\epsilon_0 r_{ij}} + A_{ij} \exp(-B_{ij} r) - \left(\frac{C_{ij}}{r_{ij}^6} + \frac{D_{ij}}{r_{ij}^9} \right) + D \{ \exp[-2\alpha(r - r_0)] - 2 \exp[-\alpha(r - r_0)] \} \quad (1)$$

where potential parameters, A_{ij} , B_{ij} , C_{ij} , D_{ij} and r_{ij} are associated between an ion i and another ion j . D and α are the depth and the shape of this potential and r_0 is the anion-cation bond length. The first term of Eq. (1) represents the Coulomb interaction. Other terms stand for short range interactions. The second term is the repulsive potential, the third one is the van der Waals interaction and the fourth one is Morse potential. Among these terms, the Coulomb interaction is dominant. In Eq. (1), z_i is the effective charge of an ion i , and 59% was assumed in the present study.

The potential parameters of U-U, U-O and O-O were determined by comparing with literature data of lattice expansion and bulk modulus. Thermal expansion of UO₂ has been reviewed by Fink.¹⁾ Calculated thermal expansion values which were changed into LTE values are shown in **Fig. 1** and were in good agreement with reported data and the experimental data of the present study. Bulk modulus was derived from compressibility. Cell volume was calculated as a function of pressure. Whole volume data were fitted to the Birch-Murnaghan equation of state. The obtained bulk modulus was 197GPa. Reported bulk modulus was around 210 GPa.⁶⁻⁸⁾ In addition, the melting point was also adjusted to 3100 K. A melting point was evaluated from an internal energy change to a temperature. An internal energy shows discontinuously change around a melting point. The potential parameters used in this study are summarized in **Table 1**.

2. Simulation Procedure and Introduction of Defect Structure

The supercell of UO₂ was prepared which consisted of a 10 x 10 x 10 fluorite unit cell structured with 12,000 ions. For the simulation, temperature was controlled with a Nose-thermostat. The step-time was 0.5x10⁻¹⁵ s/step. MD simulations were done for 5x10⁴ steps following the 5x10⁴

Table 1 Potential parameters of UO₂ fluorite structure

Ion pair	A_{ij} [J]	B_{ij} [1/Å]	C_{ij} [JÅ ⁶]	D_{ij} [JÅ ⁸]
U-O	1.670x10 ⁻¹⁵	4.186	1.598x10 ⁻²¹	0
U-U	0	5.000	0	0
O-O	9.671x10 ⁻¹⁴	5.609	1.498x10 ⁻¹⁷	0

Ion pair	D [J]	α [1/Å]	r_0 [Å]
U-O	1.50x10 ⁻²⁰	2	2.37
U-U	0	2	1.81
O-O	0	2	1.71

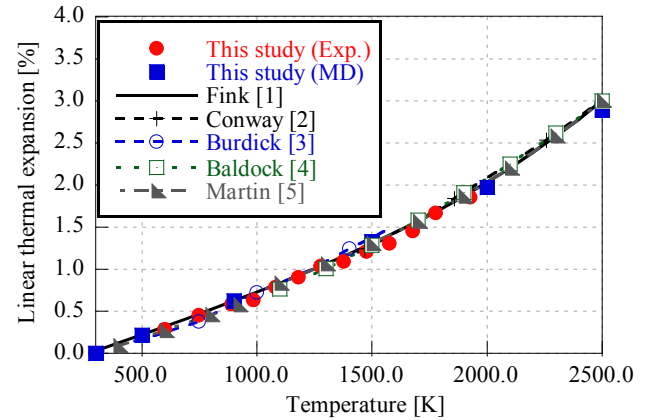


Fig. 1 Linear thermal expansion (LTE) of UO₂

steps of the initial relaxation calculation in the *NPT* ensemble.

A supercell for MD simulation is a perfect lattice and it does not contain any defects. On the other hand, the pellet of UO₂ which was prepared for the measurements included some defects and grain boundaries which would affect thermal properties. Therefore, Schottky defect was focused as one of effect factor in this study. Supercells containing Schottky defects were prepared for the simulation. One Schottky defect consisted of vacancies of one U ion and two O ions in the present study. Three types of supercells were used: a perfect lattice, a lattice containing a Schottky defect concentration of 0.25% and a lattice containing a Schottky defect concentration of 0.5%.

IV. Results and Discussion

1. Thermal Expansion

Results of thermal expansion measurement are shown in **Fig. 1**. In this temperature range, the thermal expansion values agreed with MD results and reported studies of bulk expansion measurements and lattice expansion obtained from high temperature X-ray diffraction measurement.²⁻⁵⁾ The reference data given by Conway et al. and Burdick and Parker are bulk expansion values.^{2,3)} The data of Conway is in high temperature region and the data of Burdick and Parker is in low temperature region. The reference data given by Baldock et al. is a lattice expansion value.⁴⁾ The reference data given by Martin are plotted his equations obtained from reported bulk expansion values and lattice expansion values.⁵⁾ It is consistent with many data. The measured thermal expansion values of the present study and MD thermal expansion values were fitted to Eq. (2) and Eq. (3).

$$Y = 1.574 \times 10^{-10} T^3 - 3.495 \times 10^{-7} T^2 + 1.234 \times 10^{-3} T - 3.481 \times 10^{-1} \quad (2)$$

$$Y = 2.845 \times 10^{-11} T^3 + 1.252 \times 10^{-8} T^2 + 9.985 \times 10^{-4} T - 2.989 \times 10^{-4} \quad (3)$$

where Y is the linear thermal expansion and T is the temperature in K.

It is often said that bulk expansion is higher than lattice expansion above around 1000 K because Schottky defects

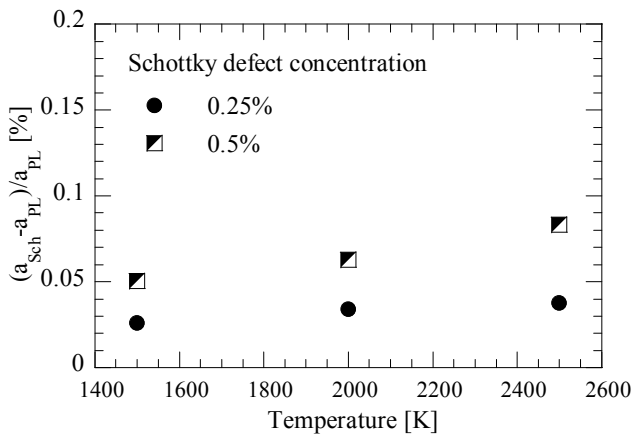


Fig. 2 Calculations of lattice parameters of UO_2 contained Schottky defects

generated thermally with increasing temperature. Therefore, the two supercells containing Schottky defects were used for the MD simulation. MD simulation results of lattice expansion are shown in **Fig. 2**. a_{Sch} is a lattice parameter of the cell containing Schottky defects and a_{PL} is a lattice parameter of the perfect lattice cell. Lattice parameters became larger values with increasing temperature and Schottky defect concentration. Martin reviewed thermal expansion data obtained from bulk expansion measurements and lattice parameter measurements.⁵⁾ He suggested that the contribution to the bulk expansion from Schottky defects was negligible, based on comparison of bulk expansion with lattice expansion. The difference in the bulk expansion by Conway et al. or the difference from the polynomial calculated by Martin to the lattice expansion by Baldock et al. was $10^{-4}\%$ to $10^{-3}\%$ in temperature range 1500 K to 2500 K.^{2,4)} Comparison of the values obtained from the MD simulation with experimental data showed that the contribution from Schottky defects was evaluated excessively by the MD simulation.

2. Specific Heat

The molar specific heat at the constant pressure, C_p , is needed to compare the experimental specific heat with the simulated specific heat. The C_p was evaluated by adding the lattice dilation term, C_d , the Schottky term, C_{Sch} and the small polaron term, C_{sp} to the molar specific heat at the constant volume, C_v . The C_v was calculated from the variation of the internal energy with respect to temperature. The C_d was given by $(3\alpha)^2 VT/\beta$, where V is the molar volume, α is the linear thermal expansion coefficient, and β is the compressibility. The values of α and β were also calculated by MD simulation. The effects of Schottky defects were evaluated by comparing simulated C_v and C_d of the perfect lattice and the defect lattices.

The MD simulation results of (a) linear thermal expansion coefficient, α , (b) compressibility, β , (c) C_v , C_d , and C_v+C_d (d) $C_v+C_d+C_{\text{Sch}}+C_{\text{sp}}$ are shown in **Fig. 3**. Schottky defects had only slight effects on α and β and so negligible. Therefore, Schottky defects also had only slight effects on

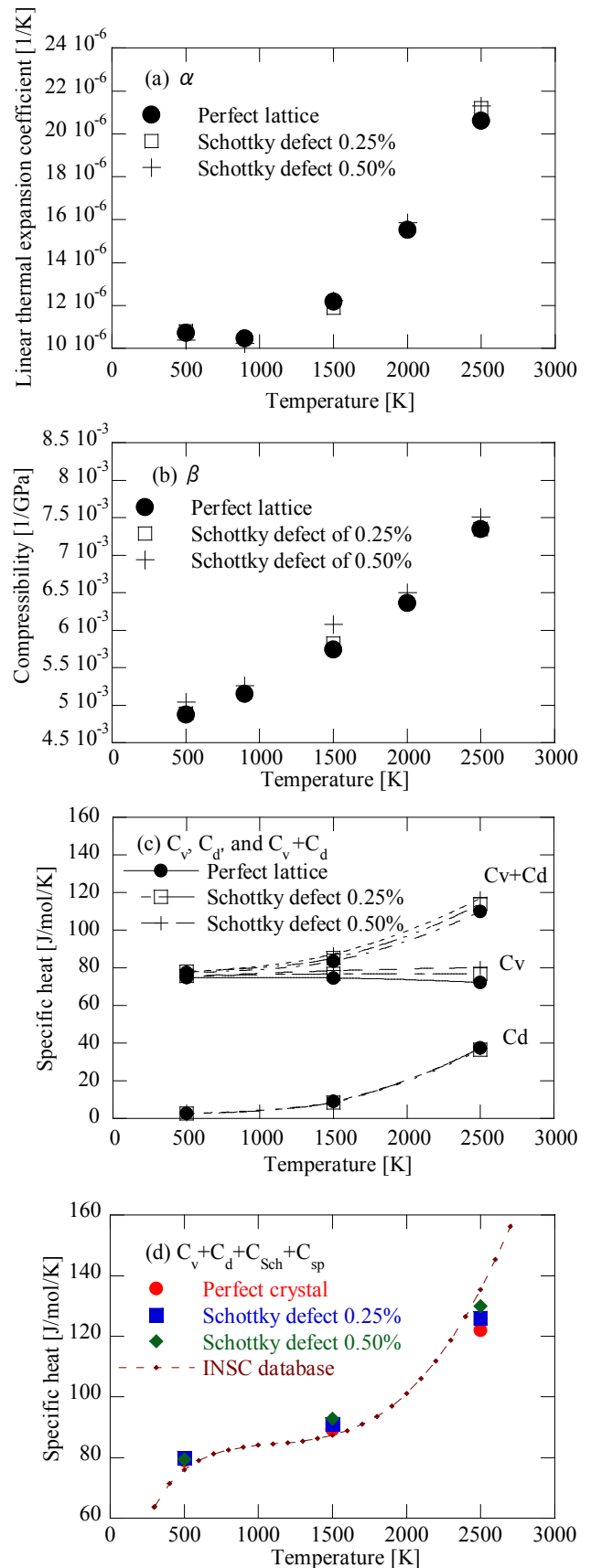


Fig. 3 The MD simulation results of (a) Linear thermal expansion coefficient, α , (b) Compressibility, β , (c) C_v , C_d , and C_v+C_d and (d) $C_v+C_d+C_{\text{Sch}}+C_{\text{sp}}$

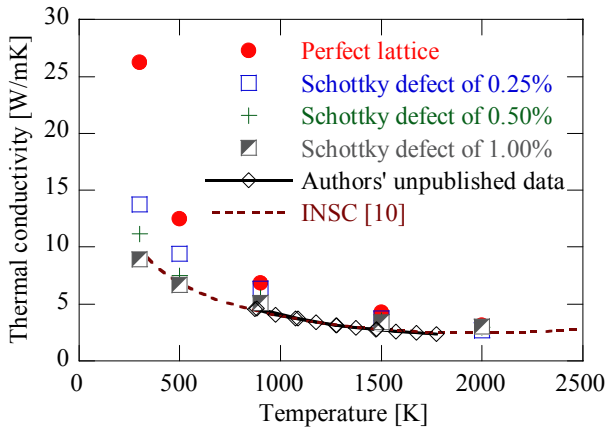


Fig. 4 Simulated thermal conductivity and experimental data of UO₂

C_d which was derived from α and β . On the other hand, C_v increased with increasing Schottky defect concentration. It seemed that increasing internal energy caused by Schottky defects had an influence on C_v . In **Fig. 3(d)**, C_{Sch} and C_{sp} were obtained from Hyland and Ralph, because they were not simulated by the present MD simulation.⁹⁾ C_{Sch} is attributed to excitation of the 5f-electron. C_{sp} is attributed to localization of electric charge of the cation which originated from a lattice strain. C_{Sch} and C_{sp} increased with temperature. In the case of increasing Schottky defects concentration with temperature, $C_v + C_d + C_{Sch} + C_{sp}$ value increased and approached roughly INSC database value.¹⁰⁾

3. Thermal Conductivity

Thermal conductivity was calculated by the Non-Equilibrium MD (NEMD) simulation. In this simulation, dynamics of the particles in the simulated cell is governed by the following equations of motion:

$$\frac{d\vec{q}_i}{dt} = \vec{v}_i \quad (4)$$

$$\frac{d\vec{p}_i}{dt} = \vec{F}_i + \vec{D}_i \vec{F}_{ext}(t) \quad (5)$$

where \vec{q}_i and \vec{p}_i are the generalized coordinate and momentum of i -th particle, \vec{v}_i is the velocity, \vec{F}_i is the force, \vec{F}_{ext} is the perturbed external force field parameter coupled with \vec{D}_i the tensor parameter. \vec{D}_i means the deviation energy of the i -th particle from the average energy in the N -particle system. For $\vec{F}_{ext} = (F_{ext}, 0, 0)$, the thermal conductivity in the x direction is written by

$$\kappa = \lim_{F_{ext} \rightarrow 0} \lim_{t \rightarrow \infty} \frac{\langle \vec{j}_E(t) \rangle}{VTF_{ext}} \quad (6)$$

Therefore, in the NEMD simulation, the thermal conductivity is defined as the proportional constant between the time-averaged energy current (heat flux) and the perturbed

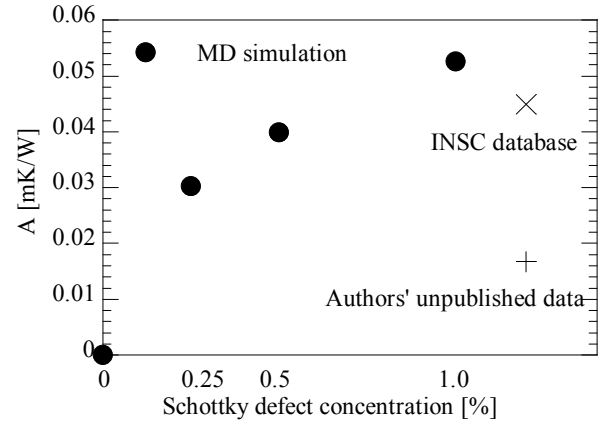


Fig. 5 Values of A obtained by MD simulation and experimental data

external force field parameter. In the above equations, $\vec{j}_E(t)$ is generally written by

$$\vec{j}_E(t) = \sum_{i=1}^N \left[\frac{m_i v_i^2}{2} + \frac{1}{2} \sum_{j \neq i} U(r_{ij}) \right] \vec{v} + \frac{1}{2} \sum_{i=1}^N \vec{v}_i \cdot \vec{r}_{ij} \vec{F}_{ij} \quad (7)$$

The energy current in the Coulomb system for the present study was given by Bernu and Vieillefosse.¹¹⁾

Thermal conductivities obtained by NEMD simulation are shown in **Fig. 4**. Some of the plotted data were the authors' unpublished experimental work corrected for porosity of 0%. Simulated values for the perfect lattice were larger than experimental data over the whole temperature range. This was attributed to the perfect lattice not containing any factors, e.g. lattice defects, grain boundaries, impurities, etc. which would decrease thermal conductivity. On the other hand, the simulated values for the supercells containing Schottky defects decreased with increasing Schottky defect concentration. It was considered that vacancies of oxygen and uranium scattered phonon vibrations and thermal conductivity decreased.

The obtained thermal conductivities were fitted to the next relationship

$$\kappa = \frac{1}{A + BT} \quad (8)$$

where κ is thermal conductivity, A is lattice defect thermal resistivity and B is specific lattice thermal resistivity. The value of B was 1.58×10^{-4} m/W when A was 0. And values of B were 2.33×10^{-4} m/W in the authors' unpublished experimental data and 2.05×10^{-4} m/W in the INSC data.¹⁰⁾ The value of B obtained by MD simulation was lower than the experimental data because thermal conductivity was very high in the low temperature range.

Values of A are plotted in **Fig. 5**. Values of A obtained by MD simulation were fitted by using B of 1.58×10^{-4} m/W. Values of A increased with increasing Schottky defects.

V. Conclusions

The interatomic potential of UO₂ in MD simulation was

determined by comparing with literature data of lattice expansion, bulk modulus and melting point. Thermal expansion was evaluated experimentally and effects of Schottky defect concentration were evaluated by MD simulation. Specific heat and thermal conductivity were also evaluated by MD simulation.

(1) Thermal Expansion

The obtained linear thermal expansion (LTE) was in good agreement with MD thermal expansion and literature data. The difference between bulk expansion and lattice expansion which was attributed to Schottky defects was evaluated by MD simulation. The supercells containing Schottky defect concentrations of 0.25% and 0.50% were prepared. Comparison of LTE of the supercells containing Schottky defects with the perfect cell showed that LTE increased with increasing Schottky defects concentration. However, it was extremely small and the effect of Schottky defects was negligible.

(2) Specific Heat

C_d and C_v were calculated by MD simulation. Schottky defects had an effect on C_v but not on C_d . It was considered that increasing internal energy was attributed to Schottky defects and C_v increased. C_{Sch} and C_{sp} were obtained from reported data. The values of $C_v+C_d+C_{Sch}+C_{sp}$ increased and approached roughly literature data with increasing Schottky defect concentration.

(3) Thermal Conductivity

Calculated thermal conductivity for the perfect lattice was higher than the experimental. This was because the perfect lattice cell did not contain any factors which would decrease thermal conductivity. Thermal conductivity de-

creased with increasing Schottky defects concentration.

References

- 1) J. K. Fink, "Thermophysical properties of uranium dioxide," *J. Nucl. Mater.*, **279**, 1-18 (2000).
- 2) J. B. Conway, R. M. Finckel, R. A. Hein, "The thermal expansion and heat capacity of UO_2 to 2200° C," *Trans. Am. Nucl. Soc.*, **6**, 153 (1963).
- 3) M. D. Burdick, H. S. Parker, "Effect of particle size on bulk density and strength properties of uranium dioxide specimens," *J. Am. Ceram. Soc.*, **39**, 181 (1956).
- 4) P. J. Baldock, W. E. Spindler, T. W. Baker, "The X-ray thermal expansion of near-stoichiometric UO_2 ," *J. Nucl. Mater.*, **18**, 305-313 (1966).
- 5) D. G. Martin, "The thermal expansion of solid UO_2 and (U, Pu) mixed oxides- a review and recommendation," *J. Nucl. Mater.*, **152**, 94-101 (1988).
- 6) V. Roque, B. Cros, D. Baron, P. Dehaut, "Effects of the porosity in uranium dioxide on microacoustic and elastic properties," *J. Nucl. Mater.*, **277**, 211-216 (2000).
- 7) M. Idiri, T. L. Bihan, S. Heathman, J. Rebizant, "Behavior of actinides under pressure: UO_2 and ThO_2 ," *Phys. Rev.*, **B70**, 014113 (2004).
- 8) S. Li, R. Ahuja, B. Johansson, "High pressure theoretical studies of actinide oxides," *High Press. Res.*, **22**, 471-474 (2002).
- 9) G. J. Hyland, J. Ralph, *High Temp. -High Press.*, **15**, 179 (1983).
- 10) International Nuclear Safety Centre (INSC) Materials Properties Database, <http://www.insc.anl.gov/matprop/>
- 11) B. Bernu, P. Vieillefosse, "Transport coefficients of the classical one-component plasma," *Phys. Rev.*, **A18**, 2345-2355 (1978).